

SymRTLO: Enhancing RTL Code Optimization with LLMs and Neuron-Inspired Symbolic Reasoning

Yiting Wang^{*1} Wanghao Ye^{*1} Ping Guo^{*2} Yexiao He^{*1} Ziyao Wang¹ Yexiao He¹ Bowei Tian¹ Shwai He¹
Guoheng Sun¹ Zheyu Shen¹ Sihan Chen³ Ankur Srivastava¹ Qingfu Zhang² Gang Qu¹ Ang Li¹

Abstract

Optimizing Register Transfer Level (RTL) code is crucial for improving the efficiency and performance of digital circuits in the early stages of synthesis. Manual rewriting, guided by synthesis feedback, can yield high-quality results but is time-consuming and error-prone. Most existing compiler-based approaches have difficulty handling complex design constraints. Large Language Model (LLM)-based methods have emerged as a promising alternative to address these challenges. However, LLM-based approaches often face difficulties in ensuring alignment between the generated code and the provided prompts. This paper introduces SymRTLO, a neuron-symbolic framework that integrates LLMs with symbolic reasoning for the efficient and effective optimization of RTL code. Our method incorporates a retrieval-augmented system of optimization rules and Abstract Syntax Tree (AST)-based templates, enabling LLM-based rewriting that maintains syntactic correctness while minimizing undesired circuit behaviors. A symbolic module is proposed for analyzing and optimizing finite state machine (FSM) logic, allowing fine-grained state merging and partial specification handling beyond the scope of pattern-based compilers. Furthermore, a fast verification pipeline, combining formal equivalence checks with test-driven validation, further reduces the complexity of verification. Experiments on the RTL-Rewriter benchmark with Synopsys Design Compiler and Yosys show that SymRTLO improves power, performance, and area (PPA) by up to 43.9%, 62.5%, and 51.1%, respectively, compared to the state-of-the-art methods.

^{*}Equal contribution ¹Department of Electrical Engineering, University of Maryland, Maryland, United States ²Department of Computer Science, City University of Hong Kong, Hong Kong ³Viterbi School of Engineering, University of Southern California, United States. Correspondence to: Ang Li <angliece@umd.edu>.

1 Introduction

Register Transfer Level (RTL) optimization is a cornerstone of modern circuit design flows, serving as the foundation for achieving optimal Power, Performance, and Area (PPA). As the earliest phase in the hardware design lifecycle, RTL development provides engineers with the most significant degree of flexibility to explore design patterns, make architectural trade-offs, and influence the overall design quality (Chu, 2006). Engineers use hardware description languages (HDLs) like Verilog to describe circuit functionality. At this stage, decisions made have far-reaching implications, as the quality of the RTL implementation directly impacts subsequent stages, including synthesis, placement, and routing (Wang et al., 2009). A well-optimized RTL not only ensures better design outcomes but also prevents suboptimal designs from propagating through the flow, which can lead to significant inefficiencies and costly iterations (Fang et al., 2023; Zhou et al., 2002).

Despite its importance, RTL optimization remains a challenging and labor-intensive task. Engineers must iteratively refine their designs through multiple rounds of synthesis and layout feedback to ensure functionality and meet stringent PPA targets. This process becomes increasingly cumbersome as design complexity grows, with synthesis times scaling disproportionately, often taking hours or even days for a single iteration. (Fang et al., 2023) Consequently, designers frequently face numerous synthesis cycles to evaluate trade-offs and reach acceptable results. While modern electronic design automation (EDA) tools provide compiler-based methods to aid optimization, these approaches are inherently limited. (Yao et al., 2024) They rely heavily on predefined heuristics, making them ill-suited for adapting to unconventional design patterns, complex constraints, or dynamic optimization scenarios. As a result, the RTL optimization process demands significant expertise and effort.

Recent advances in artificial intelligence, particularly the advent of large language models (LLMs), have introduced a new paradigm for automating and optimizing RTL code. Leveraging the powerful generative capabilities of LLMs, researchers have demonstrated their potential to rewrite and optimize Verilog code automatically (Yao et al., 2024). However, existing LLM-based approaches face critical challenges that limit their effectiveness. First, these models

often fail to align their generated outputs with specified optimization objectives. The inherent limitations in logical reasoning within LLMs can lead to deviations from intended transformations, resulting in suboptimal or incorrect outputs. Second, despite their potential for automating code generation, current methods still heavily rely on traditional synthesis feedback loops for optimization. This reliance results in the inefficiencies of the synthesis process, failing to address the core issue of long design cycles.

Our Proposed Framework. To address the critical challenges in RTL optimization, we introduce SymRTLO, the first neuron-symbolic system that seamlessly integrates LLMs with symbolic reasoning to optimize RTL code. SymRTLO significantly reduces the reliance on repeated synthesis tool invocations and enhances the alignment of LLM-generated results with intended optimization rules.

Designing such a system introduces significant challenges, which we address through the integration of carefully designed modules. The first challenge lies in the *generalization* of optimization rules. Traditionally, optimization patterns are scattered across code samples, books, and informal notes, making it difficult for compiler-based methods to formalize or apply them effectively. SymRTLO tackles this by employing an LLM-based rule extraction system, combined with a retrieval-augmented generation (RAG) mechanism and a search engine. This ensures that optimization rules are not only generalized but also efficiently retrievable from a robust library built from diverse sources.

Another critical challenge is the *alignment* of LLM-generated RTL code with the intended transformations, as LLMs often struggle to produce outputs that strictly adhere to the specified optimization objective, leading to unreliable and unexplainable results. To ensure alignment, SymRTLO employs Abstract Syntax Tree (AST)-based templates, which guide the LLM to generate code that satisfies syntactic and semantic correctness. For complex control flows or edge cases that exceed the capabilities of AST templates, the framework utilizes a symbolic generation module, designed to handle such scenarios dynamically while maintaining optimization quality.

In addition to alignment, *conflicts* often arise when different design patterns are required to meet distinct PPA goals. To address this, SymRTLO introduces a goal-oriented approach, where each optimization rule is explicitly tied to its intended objective. This enables selective application based on user-defined optimization goals, efficiently balancing these conflicts to deliver optimized designs without disproportionately compromising PPA metrics.

Verification Traditional RTL verification requires extensive manual test case creation. To address this, SymRTLO integrates an automated test case generator, streamlining verification while ensuring functional correctness.

Our key contributions are summarized as follows:

1. **LLM Symbolic Optimization:** SymRTLO, the first framework to combine LLM-based rewriting with symbolic reasoning for RTL optimization.
2. **Data Path and Control Path Optimization:** SymRTLO addresses critical challenges in both traditional EDA compilers and purely LLM-based approaches, particularly by aligning generated code with FSM and data path algorithms, balancing conflicting optimization rules, and improving explainability.
3. **PPA Improvements:** SymRTLO demonstrates its efficacy on industrial-scale and benchmark circuits, surpassing manual coding, classical compiler flows (e.g., Synopsys DC Compiler), and state-of-the-art LLM-based methods, achieving up to 43.9%, 62.5%, and 51.1% improvements in power, delay, and area.

2 Background and Motivation

LLMs have emerged as powerful tools for RTL design automation, with various approaches being developed since 2023. As summarized in Table 1, these approaches fall into three primary categories: *RTL code generation* (Liu et al., 2023a; 2024; Chang et al., 2023; Blocklove et al., 2023), *debugging* (Tsai et al., 2024), and *optimization* (Yao et al., 2024). This growing body of research demonstrates the significant potential of LLMs to improve the efficiency and effectiveness of EDA workflows. However, RTL code optimization has always been a significant challenge in RTL design, even for human experts, as it has the greatest impact on the performance of downstream tasks.

Challenges in RTL Code Optimization with LLMs.

Aligning generated code with intended optimization goals is a major challenge in LLM-based RTL optimization. Due to inherent randomness, LLMs often produce incomplete, incorrect, or suboptimal results. For example, RTL-Rewriter (Yao et al., 2024) employs retrieval-augmented prompts and iterative synthesis-feedback loops to enhance functional correctness but still struggles with fundamental misalignment between generated code and optimization objectives. Additionally, the need for multiple synthesis rounds significantly increases optimization time as design complexity increases, limiting the scalability of current LLM-based methods for large industrial-scale designs.

Current Approaches: Underutilization of Knowledge and Manual Verification. Traditional RTL design optimization relies on established patterns such as subexpression elimination (Pasko et al., 1999; Cocke, 1970), dead code elimination (Knoop et al., 1994; Gupta et al., 1997), strength reduction (Cooper et al., 2001), algebraic simplification (Buchberger & Loos, 1982; Carette, 2004), Mux reduction (Chen & Cong, 2004; Wang et al., 2023), and memory sharing (LaForest & Steffan, 2010; Ma et al., 2020). While these techniques are effective, these optimizations

Table 1. Comparative analysis of LLM-based methods for RTL design. ✓ indicates the presence of the feature, while ✗ indicates absence of the feature.

Category	Method	Verification Capability	Rule-Based	Output Alignment	Conflict Resolution
Generation	ChipNeMo (Liu et al., 2023a)	✗	✗	✗	✗
	VeriGen (Thakur et al., 2024)	✗	✗	✗	✗
	VerilogEval (Liu et al., 2023b)	✗	✗	✗	✗
	RTLCoder (Liu et al., 2024)	✗	✗	✗	✗
	ChipChat (Blocklove et al., 2023)	✗	✗	✗	✗
	ChipGPT (Chang et al., 2023)	✗	✗	✗	✗
Debug	RTLFixer (Tsai et al., 2024)	✓	✓	✗	✗
Optimization	RTLRewriter (Yao et al., 2024)	✓	✓	✗	✗
	SymRTLO (Ours)	✓	✓	✓	✓

typically operate at the gate-level netlist, making the relationship between optimized output and original RTL code less transparent. Additionally, optimization patterns from design manuals and codebases remain underutilized due to the lack of a centralized repository, forcing engineers to rely on their expertise rather than automated tools. Furthermore, verification requires the creation of test benches and test cases manually, making the RTL design flow both time-consuming and error-prone.

Table 2. Conflicts Between Design Goals & Optimization Patterns.

Design Pattern	Goal	Conflict Goal	Conflict Design Pattern
Pipelining	Low Timing	Low Area	Resource Sharing
Clock Gating	Low Power	Low Timing	Retiming

Optimization Conflicts and Limited Compiler Capabilities. Existing compiler-based methods face additional challenges, particularly in managing **optimization goal conflicts** and handling complex patterns. For instance, optimizing for one metric, such as delay, often conflicts with another, such as power consumption. Striking the right balance between these competing objectives is crucial, especially as trade-offs between power and delay directly impact overall system performance. As shown in Table 2, each optimization method has its own specific goal, which often clashes with others. Compiler-based methods also lack the flexibility to adapt to such conflicts, limiting their effectiveness in optimizing designs with diverse and competing constraints.

Advancing LLM-based RTL Optimization with Neuro-Symbolic Integration. Recent research has shown a growing trend toward combining symbolic reasoning with LLM (Yang et al., 2023; Wan et al., 2024b; Diego Calanzone & Vergari, 2024; Deepa Tilwani & Sheth, 2024; Wan et al., 2024a), bringing new inspirations for more efficient and reliable LLM-based RTL code optimization with better prompt-code alignment. These integrated approaches have seen broad application across various fields, from automated theorem proof and knowledge representation to robotics and medical diagnostics, demonstrating how the combination of pattern recognition and generative capabilities of LLM with the interpretability and logical rigor of symbolic sys-

tems can significantly improve the alignment between LLM output and the given prompt.

Motivation Experiments. To highlight the limitations of current LLM-based RTL optimization, we conduct an experiment using state-of-the-art commercial LLM, GPT-O1, to optimize an 11-state FSM design. The goal was to minimize and merge unnecessary states to enhance PPA metrics. GPT-O1 receives a detailed state reduction algorithm to guide the optimization process. We compare its results with an optimized design that directly applied the state reduction algorithm. As shown in Table 3, GPT-O1 struggles to align its outputs with the algorithm, resulting in an under-optimized FSM with minimal state reduction and improvement in PPA. In contrast, algorithm-driven optimization achieves significantly better results, underscoring the challenges LLM-based methods face in handling complex optimization tasks.

Table 3. Performance Comparison Across Different Approaches.

Approach	# States	Time (ns)	Power (mW)	Area (μm^2)
Baseline	11	0.041	2.250	833.000
GPT-O1	10	0.041	2.280	993.480
Optimized	4	0.025	1.170	403.920

3 Methodology

SymRTLO takes a Verilog RTL module as input and optimizes it for specific design goals, such as low power, high performance, or reduced area. As illustrated in Figure 1, the workflow begins by entering the RTL code and the user-specified optimization goal (①) into the **LLM Dispatcher** (②). This dispatcher analyzes the input circuit and determines the appropriate optimization path: either proceeding solely with **Data Flow Optimization** (§3.2) or incorporating **Control Flow Optimization** (§3.3) as well, depending on the characteristics of the design. For Data Flow Optimization, a search engine with a retrieval-augmented module extracts optimization rules and constructs AST-based templates. For Control Flow Optimization, an LLM-driven symbolic system generator performs FSM-specific transformations. Finally, the **Final Optimization Module** (§3.4) integrates both paths and incorporates a verification system to ensure the functional correctness of the optimized design.

3.1 LLM Dispatcher

The **LLM Dispatcher** (②) receives the input RTL code and the specified optimization goal (e.g., low power) (①) before any optimization begins. It first summarizes the code and generates potential optimization suggestions. These suggestions are then passed to the Retrieval-Augmented Generation (RAG) system to identify the relevant optimization rules. Additionally, the Dispatcher evaluates the presence of a Finite State Machine (FSM) in the original code to determine whether control flow optimization is necessary.

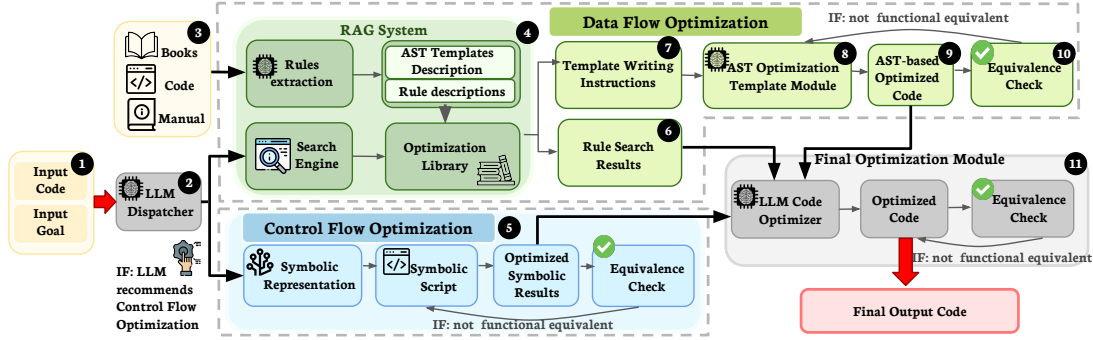


Figure 1. SymRTLO Architecture.

3.2 Data Flow Optimization

Data Flow represents the process by which information is propagated, processed, and optimized within an RTL design. Effective data flow optimizations improve system efficiency by simplifying computations, reducing redundancy, and enhancing PPA metrics. Common techniques include sub-expression elimination, constant folding, and resource sharing. The proposed Data Flow Optimization Module addresses three key challenges: (1) generalizing diverse optimization patterns into accurate, reusable rules; (2) aligning LLM-generated optimizations with functional and logical requirements; and (3) resolving conflicts between optimization goals inherent in distinct design patterns.

Optimization Rule Search Engine Optimization knowledge is often scattered across books, lecture notes, codebases, and design manuals, with no generalized repository to serve as a unified knowledge base. Furthermore, optimization patterns frequently *conflict* due to divergent goals, for example, power reduction versus performance improvement. To tackle these challenges, we developed a retrieval-augmented generation (RAG) system equipped with an optimization goal-based rule extraction module.

Optimization Library. The RAG system aggregates raw RTL optimization data from sources such as lecture notes, manuals, and example designs (Vahid, 2010; Taraate, 2022; Schultz, 2023; Palnitkar, 2003) into a comprehensive knowledge base (3). LLMs then summarize and structure these data into an optimization library (4). Each rule is abstracted to include its description, applicable optimization goals (e.g., area, power, or timing), and its category (e.g., data flow, FSM, MUX, memory, or clock gating). A similarity engine identifies overlaps with existing entries, prompting merges or exclusive labels to ensure the scalability of the rule library. To align optimization goals with generated outputs, the rules specify detailed instructions for constructing AST templates, enabling precise application of optimization patterns. Rules with clearly defined requirements include template-writing guidelines, while more abstract rules are

stored as descriptive text and used directly as optimization prompts. An example RAG is included in Appendix C.

Enforcing Rule Alignment and Resolving Conflicts To improve the structure and alignment of optimization rules, the LLM Dispatcher (1) provides both a summary of the input RTL code and suggestions for potential optimizations. These inputs are passed to the search engine along with user-specified optimization goals, performing a similarity search to identify the most relevant rules from the RAG system.

Given the potential for conflicts between optimization goals, it is critical to prevent the inclusion of conflicting rules while ensuring no critical optimizations are overlooked. To achieve this balance, we employ the elbow method to analyze the similarity scores between the query and the candidate rules. This approach identifies a natural cutoff point where adding more rules no longer yields significant benefits. Let the similarity scores between the query and candidate rules be ordered as:

$$s_1 \geq s_2 \geq \dots \geq s_M, \quad (1)$$

where s_i denotes the similarity score for i -th rule, ordered from highest to lowest, and M is the total number of candidates. The optimal cutoff index i^* is determined by maximizing the difference between consecutive similarity scores:

$$i^* = \arg \max_{1 \leq i < M} (s_i - s_{i+1}). \quad (2)$$

Rules with similarity scores above the threshold τ_{elbow} are selected for application. The similarity between the query embedding ($\mathbf{e}_{\text{query}}$) and the a rule embedding (\mathbf{e}_{rule}) is computed as shown below:

$$\text{sim}(\mathbf{e}_{\text{query}}, \mathbf{e}_{\text{rule}}) = \frac{\mathbf{e}_{\text{query}} \cdot \mathbf{e}_{\text{rule}}}{\|\mathbf{e}_{\text{query}}\| \|\mathbf{e}_{\text{rule}}\|} \geq \tau_{\text{elbow}}. \quad (3)$$

This method ensures that only the most relevant rules are selected, striking an optimal balance between comprehensiveness and precision. The output of the search engine contains two components: rules with detailed template-writing instructions (7) and abstract rules described only by their optimization properties (6).

AST Template Building To ensure that LLM-generated RTL code aligns with functional and logical optimization goals, we enforce rules using AST-based symbolic systems, which have been proven to be effective in hardware debugging (Tsai et al., 2024). Compared to LLM-generated symbolic systems, AST-based templates offer several advantages: (1) parsing Verilog into an AST ensures accurate and structured design representations; (2) limiting each template to a single optimization goal maintains conciseness, facilitating correct generation and application by LLMs; and (3) the modular approach allows selection of templates to balance conflicting optimization patterns, enhancing flexibility.

For rules that include template-writing instructions, we prompt the LLM to generate an AST-based template that serves as a general optimization framework (⑧). Let \mathcal{A} denote the set of all AST nodes in the Verilog design, and let the matching condition:

$$\Phi : \mathcal{A} \rightarrow \{\text{true}, \text{false}\}, \quad (4)$$

determine whether a node qualifies for optimization. The process begins by identifying the **Target Node Type**, such as Always, Instance, Assign or Module Instantiation. For each node of the specified type, we apply Φ to decide whether it requires rewriting. Once the target nodes are identified, the **Transformation Rule** is applied as follows:

$$\tau : \{a \in \mathcal{A} \mid \Phi(a) = \text{true}\} \longrightarrow \mathcal{A}, \quad (5)$$

where τ replaces the matched node with an optimized AST subtree (e.g., merging nested `if-else` statements, folding constants, or simplifying expressions; code example see Appendix B). To ensure functional correctness, the transformed design undergoes an equivalence check using LLM-generated testbenches. If the template passes verification, it is stored in the RAG system as reusable content.

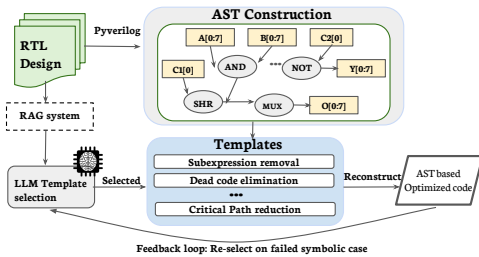


Figure 2. SymRTLO AST template optimization workflow.

As shown in Figure 2, the RTL design is initially interpreted as an AST representation. The RAG system provides the LLM with multiple template options. Due to the varying optimization goals and scenarios, the system avoids relying on a fixed sequence of templates. Instead, the LLM determines which templates to apply and in what order, tailoring the

optimization process to the design’s specific requirements. To further prevent conflicts between templates or failures in the symbolic system, we introduce a **feedback loop**. This loop allows the LLM to re-select templates and adjust its strategy based on prior failures, ensuring robustness and adaptability in the optimization process.

3.3 Control Flow Optimization

Control Flow, unlike Data Flow’s focus on how information is processed and propagated, defines the execution paths and sequencing of operations in RTL designs through finite-state machines (FSMs) that capture states, transitions, and outputs. These FSMs are tightly coupled with design constraints (*i.e.*, partial specifications, clock gating, and reset logic), making generic symbolic systems fragile or incomplete. Addressing these challenges requires deeper semantic analysis beyond simple pattern matching or generic AST templates. To enhance alignment between optimized code and the FSM minimization algorithm, we propose a Control Flow Optimization module utilizing an LLM-based symbolic system. An FSM can be formally represented as:

$$M = (Q, \Sigma, \delta, q_0, F), \quad (6)$$

where Q is the finite set of states, Σ is the input alphabet, $\delta : Q \times \Sigma \rightarrow Q$ is the transition function, $q_0 \in Q$ is the initial state, and $F \subseteq Q$ is the set of accepting states.

For a partially specified FSM M_p , the transition function is extended to handle non-deterministic transitions:

$$\delta_p : Q \times \Sigma \rightarrow 2^Q, \quad (7)$$

where 2^Q represents the power set of Q .

Classical minimization algorithms (*e.g.*, Hopcroft’s (Hopcroft & Ullman, 1969) or Moore’s (Moore et al., 1956)) are effective for fully specified deterministic FSMs but are limited by real-world complexities. Practical RTL designs often integrate control logic with data path constraints, and undefined states and transitions make FSM minimization an NP-complete problem with a general complexity of $O(2^{|Q|})$. A single pre-built AST script cannot efficiently handle all such partial specifications. Let:

$$\phi : Q \times D \rightarrow B, \quad (8)$$

represent the data path constraints, where D is the data path state space and B is the boolean domain. Pure FSM-focused AST-based optimization scripts can overlook these data path side effects, failing to capture deeper control semantics.

Inspired by (Hu et al., 2023), we propose leveraging LLMs to transform each circuit into a symbolic representation focused solely on FSM components, *i.e.*, isolating states, transitions, and relevant outputs, as illustrated in Figure 3. Instead of relying on a one-size-fits-all script, we prompt the LLM to dynamically generate a **specialized minimization**

script tailored to the specific FSM structure and constraints. The optimization is formulated as:

$$\min_{M'} f(M', C) \text{ subject to } \phi(M', D) = \text{true}, \quad (9)$$

where M' represents the optimized FSM, C represents the design constraints, and $\phi(M', D)$ ensures consistency with the data path. Appendix A shows an example workflow.

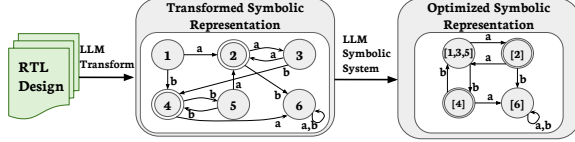


Figure 3. SymRTL0 FSM optimization workflow.

3.4 Verification and Final Optimization

To address the challenges of manual verification and unreliable automated methods, we introduce an automated verification module that integrates functionality testing and formal equivalence checking. After AST-based optimization and the LLM-assisted symbolic system generate initial results, the LLM combines extracted rules, template-optimized code, and symbolic outputs to produce the final optimized RTL design (11). Verification is essential to ensure correctness, as LLM-generated rewrites may introduce unintended behavioral deviations. We employ a two-step verification pipeline: (1) the LLM generates test benches to validate basic functional correctness, acting as a rapid filter to reject invalid rewrites early; and (2) for designs that pass initial tests, we perform satisfiability (SAT)-based equivalence checking to formally confirm functional equivalence to the original design. Although SAT-based verification is rigorous and ensures accuracy, it can be computationally expensive, particularly for complex designs with arithmetic-heavy circuits. By combining SAT checks with the quick, randomized testing from the first step, we significantly reduce the number of candidates requiring formal verification. This hybrid approach optimizes the trade-off between verification accuracy and computational cost, allowing us to efficiently validate even complex optimizations.

4 Experiments

4.1 Experimental Setup

Baseline We compare SymRTL0 with several state-of-the-art LLM and open source RTL optimization frameworks. The LLM baselines include GPT-4o, GPT-4(OpenAI et al., 2023), GPT-3.5(Ye et al., 2023), and GPT-4o-mini. Additionally, we include two specialized open-source LLM-based tools: Verigen(Thakur et al., 2024) and RTL-Coder-Deepseek (Liu et al., 2024). For a comprehensive evaluation,

we analyze 11 RTLRewriter short-benchmark examples for Wires and Cells and 10 complex FSM and algorithm examples from both short and long benchmarks for PPA. Although the RTLRewriter environment is reproducible using Yosys (Wolf et al., 2013) for wires and cells analysis, the exact test case they use is not provided. Moreover, comparing PPA results is even more challenging due to its reliance on Yosys + ABC (Brayton & Mishchenko, 2010) with unknown libraries. To demonstrate SymRTL0’s capabilities, we subject it to a broader evaluation scope, selecting examples that are diverse in size and functionality, while including cases reported in RTLRewriter’s benchmark for direct comparison.

Implementations The SymRTL0 framework relies on GPT-4o as its primary LLM for optimization strategy selection, symbolic system generation, and iterative HDL synthesis, leveraging its robust inference and coding capabilities. Other models like GPT-3.5 and GPT-O1 were excluded after preliminary experiments revealing poor performance: GPT-3.5 lacks sufficient coding capabilities, and GPT-O1 incurs high costs and long inference times, making our framework less efficient. Pyverilog (Takamaeda-Yamazaki, 2015) is used for AST extraction and code reconstruction.

To efficiently retrieve relevant transformation templates and knowledge, we integrate OpenAI’s text embedding-3-small, which excels in embedding-based retrieval tasks. For hardware compilation and validation, we use a combination of open-source and commercial tools. Yosys measures wires and cells, while Synopsys DC Compiler 2019 (Synopsys), paired with the Synopsys Standard Cell (SSC) library, performs PPA analysis. GPT-4o generates test benches for functional coverage, and Yosys + ABC serves as the logical equivalence checker. For a fair comparison with standard compiler workflows, we apply typical Synopsys DC Compiler optimizations, explicitly setting the area constraint to zero and using medium mapping effort with incremental mapping to reflect common practices.

Evaluation Metrics First, to evaluate generation quality and functional correctness, we use the pass@k metric commonly employed in code generation tasks. This metric captures the probability that at least one valid solution exists within the top k generations:

$$\text{pass@k} = \frac{1}{N} \sum_{i=0}^N \left(1 - \frac{C_{n_i - c_i}^k}{C_{n_i}^k}\right), \quad (10)$$

where N is the number of problems, n_i and c_i represent the total and correct samples for the i -th problem, respectively. Second, to test the performance of the synthesis results, we use the best results of the 10 valid generations of each model and our method. For smaller benchmarks, we evaluate optimization results using Wires and Cells ¹

Table 5. Comparison of Wire and Cell Counts. Gray highlighting denotes state-of-the-art results. GeoMean is the geometric mean of the resource usage (wires or cells). Ratios are calculated by dividing the geometric mean of resource usage by the baseline’s usage.

Benchmark	Yosys		GPT-4-Turbo		GPT-4o		GPT-3.5-Turbo		GPT-4o-mini		RTLCoder-DS		RTLrewriter		SymRTLO	
	Wires	Cells	Wires	Cells	Wires	Cells	Wires	Cells	Wires	Cells	Wires	Cells	Wires	Cells	Wires	Cells
adder_subexpression	8	3	7	3	7	3	7	3	7	3	8	3	7	3	7	3
adder_architecture	86	56	30	40	30	40	96	63	86	56	86	56	-	-	14	16
multiplier_subexpr	26	71	18	15	259	255	26	71	26	71	26	71	-	-	18	15
constant_folding_raw	12	6	10	5	10	5	10	5	10	5	12	6	-	-	8	5
subexpression_elim	17	12	19	12	19	12	19	12	17	10	17	12	-	-	14	8
alu_subexpression	30	24	30	24	28	22	30	24	27	22	30	24	21	18	21	18
adder_resource	13	3	6	3	9	4	6	3	7	3	13	3	-	-	6	3
multiplier_bitwidth	9	3	8	3	8	3	9	3	9	3	9	3	8	3	8	3
multiplier_architect	4	2	14	36	4	2	16	20	18	36	4	2	-	-	4	2
adder_bit_width	4	1	3	1	3	1	3	1	3	1	4	1	3	1	3	1
loop_tiling_raw	5	16	4	16	4	16	4	16	484	496	5	16	-	-	3	16
GeoMean	15.49	8.96	13.45	9.81	16.35	9.97	16.40	11.49	16.31	11.49	15.49	8.96	-	-	9.75	5.95
Ratio	1.00	1.00	0.87	1.10	1.06	1.11	1.06	1.28	1.11	1.31	1.15	0.91	0.69 [†]	0.77 [†]	0.63	0.67

Table 6. FSM Designs PPA Comparison. Gray highlights indicate state-of-the-art results. A \downarrow marks improvement, while a \uparrow denotes a decline compare with the original design. Two comparison scenarios are shown: without compiler optimization (upper improvement) and with compiler optimization (lower improvement). A - indicates that no code is available for analysis.

Model/Method	example1.state			example2.state			example3.state			example4.state			example5.state		
	Power (mW)	Time (ns)	Area (μm^2)	Power (mW)	Time (ns)	Area (μm^2)	Power (mW)	Time (ns)	Area (μm^2)	Power (mW)	Time (ns)	Area (μm^2)	Power (mW)	Time (ns)	Area (μm^2)
Original	0.042	1.21	833.0	0.056	2.25	549.4	0.052	1.35	589.6	0.055	2.18	597.1	0.055	2.18	597.1
GPT-3.5	0.043	1.27	870.6	0.056	2.25	549.4	0.052	1.35	589.6	0.059	2.17	972.3	0.055	2.18	597.1
GPT4o-mini	0.055	1.08	1021.1	0.062	2.23	579.2	0.063	1.08	714.9	0.055	2.18	597.1	0.053	2.18	634.7
GPT-4-Turbo	0.053	2.97	993.5	0.067	2.28	737.6	0.065	1.22	810.3	0.055	2.18	273.5	0.029	2.25	366.8
GPT-4o	0.053	2.97	1002.5	0.056	2.25	549.4	0.052	1.35	589.6	0.055	2.18	273.5	0.055	2.18	597.1
RTLCoder-DS	0.042	1.21	833.0	0.056	2.25	549.4	0.052	1.35	589.6	0.055	2.18	597.1	0.055	2.18	597.1
SymRTLO	0.047	0.36	534.4	0.024	1.17	271.0	0.023	1.15	268.5	0.024	2.17	273.5	0.026	2.18	270.9
Improvement(%)	\uparrow 11.90	\downarrow 70.25	\downarrow 35.85	\downarrow 57.14	\downarrow 48.00	\downarrow 50.67	\downarrow 55.77	\downarrow 14.81	\downarrow 54.46	\downarrow 56.36	\downarrow 0.46	\downarrow 54.1952	\downarrow 52.73	0.00	\downarrow 54.63
Original + Compiler Opt.	0.041	2.85	564.51	0.035	2.24	316.11	0.038	1.23	358.77	0.044	2.19	451.59	0.045	2.19	451.59
SymRTLO + Compiler Opt.	0.021	2.64	240.85	0.018	0.6	175.61	0.018	2.42	180.63	0.020	2.17	185.65	0.019	2.27	188.169
Improvement(%)	\downarrow 48.78	\downarrow 7.37	\downarrow 57.33	\downarrow 48.57	\downarrow 73.21	\downarrow 44.45	\downarrow 52.63	\uparrow 96.74	\downarrow 49.65	\downarrow 54.55	\downarrow 0.91	\downarrow 58.89	\downarrow 57.78	\uparrow 3.65	\downarrow 58.33

Table 4. Pass Rate Results.

Method	Pass@1	Pass@5	Pass@10
Ours	97.5	100.0	100.0
GPT-4o	45.9	60.0	72.7
GPT-4-Turbo	42.9	62.7	81.8
GPT-4o-mini	2.5	10.9	12.7
GPT-3.5-Turbo	28.6	42.7	54.5
RTLCoder DeepSeek	8.8	18.2	27.3
Verigen-2B	0.0	0.0	0.0
Verigen-16B	0.0	0.0	0.0

metrics, which reflect low-level physical characteristics of circuits. These metrics provide granular insights into routing complexity (wires) and logical component count (cells), offering a precise evaluation for isolated modules or blocks.

For larger designs, we focus on PPA metrics to capture high-level efficiency and real-world applicability. These metrics offer a holistic view of resource usage and performance for complex designs, where low-level metrics like Wires and Cells become impractical.

4.2 Functional Correctness Analysis

To demonstrate that our method reduces synthesis time and improves functional correctness, Table 4 presents the evaluation results. SymRTLO achieves near-perfect pass rates in first-attempt optimizations. This demonstrates exceptional consistency in generating valid, optimized RTL code. This significantly outperforms state-of-the-art language models, particularly given the complexity of RTL optimization tasks

[†]: Reported Results from (Yao et al., 2024).

and the necessity of maintaining functional equivalence. As a result, SymRTLO minimizes the number of synthesis iterations required, reducing redundant computations and streamlining the overall optimization process.

4.3 Circuit Optimization Performance

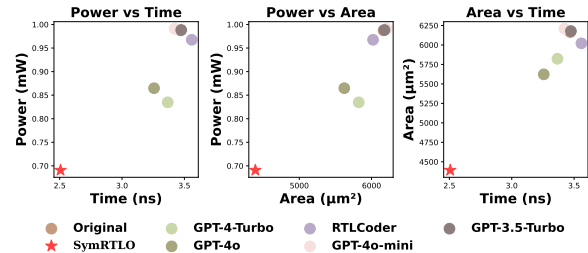


Figure 4. The PPA overall improvement of benchmark cases.

To demonstrate SymRTLO’s effectiveness in resolving cross-rule conflicts and achieving optimization objectives, we conduct an experiment presented in Figure 4. Given the limited benchmarks available for LLM-driven RTL design, we rely on RTLrewriter’s benchmark, which primarily emphasizes area optimization, leaving minimal room for improvements in power and delay. To align with this limitation, we put area optimization as our primary goal. Despite these constraints, SymRTLO achieves substantial improvements, averaging 40.96% in power, 17.02% in delay, and 38.05% in area, while maintaining a balanced optimization across all three

Table 7. Algorithm Optimizations PPA Comparison. Gray highlights indicate state-of-the-art results. A \downarrow marks improvement, while a \uparrow denotes a decline compare with the original design. Two comparison scenarios are shown: without compiler optimization (upper improvement) and with compiler optimization (lower improvement).

Model/Method	sppm_redundancy			subexpression_elim			adder_architecture			vending			fft		
	Power (mW)	Time (ns)	Area (μm^2)	Power (mW)	Time (ns)	Area (μm^2)	Power (mW)	Time (ns)	Area (μm^2)	Power (mW)	Time (ns)	Area (μm^2)	Power (mW)	Time (ns)	Area (μm^2)
Original	2.863	7.41	40102.6	5.265	11.09	10989.1	0.418	2.78	1023.5	7.61	227.86	176982.98	58.23	8.26	2255264.75
GPT-3.5-Turbo	2.863	7.41	40102.6	5.265	11.09	10989.1	0.418	2.78	1023.5	7.61	227.86	176982.98	58.23	8.26	2255264.75
GPT-4o-mini	2.863	7.41	40102.6	5.265	11.09	10989.1	0.418	2.78	1023.5	7.61	227.86	176982.98	58.23	8.26	2255264.75
GPT-4-Turbo	2.863	7.41	40102.6	3.936	11.09	7783.03	0.392	2.74	1023.5	7.50	227.86	176982.98	58.23	8.26	2255264.75
GPT-4o	2.863	7.41	40102.6	5.296	11.09	8984.61	0.392	2.74	1023.5	7.61	227.86	176982.98	58.23	8.26	2255264.75
RTLCoder-DS	2.863	7.41	40102.6	5.265	11.09	10989.1	0.418	2.78	1023.5	7.61	227.86	176982.98	58.23	8.26	2255264.75
SymRTL0	1.762	7.29	29606.18	3.018	2.87	7358.8	0.328	1.97	762.6	6.97	227.86	164831.1	31.71	8.09	1726125.71
Improvement(%)	\downarrow 38.46	\downarrow 1.62	\downarrow 26.17	\downarrow 42.68	\downarrow 74.12	\downarrow 33.04	\downarrow 21.53	\downarrow 29.14	\downarrow 25.49	\downarrow 8.41	\downarrow 0	\downarrow 6.87	\downarrow 45.54	\downarrow 2.06	\downarrow 23.46
Original + Compiler Opt.	1.46	7.95	22908.69	4.61	11.78	9484.15	0.17	2.29	541.920	11.46	7.90	240079.29	51.12	7.90	1857805.49
SymRTL0 + Compiler Opt.	1.46	7.95	22908.69	3.53	11.78	6791.88	0.17	2.48	531.880	8.175	7.90	151593.86	26.32	8.98	1471378.46
Improvement(%)	0	0	0	\downarrow 23.4	0	\downarrow 28.39	0	\uparrow 8.30	\downarrow 1.86	\downarrow 28.66	0	\downarrow 36.86	\downarrow 48.51	\uparrow 13.67	\downarrow 20.8

metrics, highlighting its versatility and robustness.

Smaller benchmarks require only 1–2 optimization patterns to optimize, making them ideal for testing *alignment* between LLM and the output to ensure our approach accurately represents the optimization patterns. Table 5 shows that SymRTL0 consistently outperforms baseline implementations across various test cases. With wire and cell ratios of 0.63 and 0.67 respectively, it surpasses the state-of-the-art values of 0.69 and 0.77. While models like GPT-4 excel in certain cases, they lack consistency across diverse optimization tasks. Even RTL-focused models, despite their specialized training, exhibit limitations in optimization tasks.

In FSM PPA experiments, SymRTL0 significantly outperforms existing approaches, particularly in relation to RTL-Rewriter, the state-of-the-art solution, achieving an improvement of up to 50.59%, 12.65%, 53.09% in power, time, and area, respectively. As shown in Table 6, it effectively aligns the FSM state reduction algorithm with optimized code, minimizing all FSM states and achieving the best overall PPA results. This demonstrates that the LLM-generated symbolic system is both stable and aligned with intended optimization goals.

To evaluate the effectiveness of generalized rules and AST templates in balancing conflicting rules, we conduct algorithm case PPA experiments involving complex Data Path and Control Path scenarios. As shown in Table 7, SymRTL0 applies AST templates, optimized rules, and minimized FSM states, achieving 30.34%, 21.37%, and 20.01% improvements in PPA over GPT-4o, our base model, on average. Since RTLRewriter’s generated code isn’t publicly available, we cannot test or compare our results.

We test SymRTL0 with Synopsys DC optimization workflows for both FSM and Algorithm cases, as shown in Table 6 and Table 7, demonstrating further balanced optimization alongside compiler optimization processes, achieving overall improvements of 36.2% in power and 35.66% in area, with only an 8.3% increase in time as a trade-off.

4.4 Ablation Studies

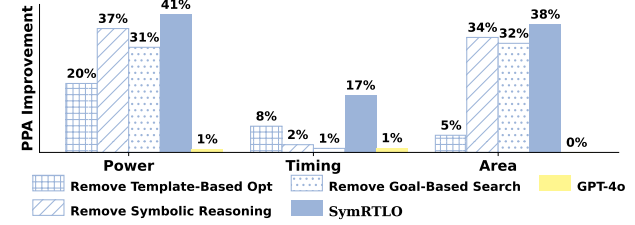


Figure 5. Ablation results.

To assess the effectiveness of individual components in SymRTL0, we conduct ablation studies by selectively removing one module at a time, *i.e.*, either the AST-based module, FSM symbolic system, or goal-based search engine, while keeping the rest of the system intact. We then analyze the impact of each removal across test cases, measuring the resulting overall PPA improvements compared to the baseline. Figure 5 summarizes these results, showing that all three components contribute significantly to SymRTL0’s overall performance. Removing any one of them results in substantial losses in optimization effectiveness, further emphasizing the necessity of their integration. By contrast, GPT-4o alone achieves minimal improvements, underscoring the advantages of SymRTL0’s tailored framework.

5 Conclusion

We present SymRTL0, a neuron-symbolic framework that integrates LLM-based code rewriting and symbolic reasoning to optimize both data flow and control flow in RTL designs. SymRTL0 generalizes optimization rules, aligns generated code with intended transformations, resolves conflicting optimization goals, and ensures reliable automated verification. By combining retrieval-augmented guidance with symbolic systems, SymRTL0 automates complex structural rewrites while maintaining functional correctness. Extensive evaluations on industrial-scale designs demonstrate significant PPA gains over state-of-the-art solutions.

Impact Statement

SymRTL0 advances EDA by integrating Large Language Models with symbolic reasoning to automate and optimize RTL code more efficiently than existing methods. This innovation not only significantly enhances PPA metrics—enabling the development of more energy-efficient and compact electronic devices—but also accelerates chip design, prototyping, and the creation of specialized chips. By reducing design time and reducing production costs, SymRTL0 facilitates faster industry growth and empowers scientific exploration through more accessible and cost-effective hardware development. Additionally, by lowering the expertise barrier and reducing the educational costs associated with chip design, SymRTL0 democratizes hardware development, allowing a broader range of engineers and even non-experts to design their own chips. This democratization fosters greater innovation, minimizes human error, and contributes to economic growth and environmental sustainability, ultimately transforming the landscape of chip production and scientific research.

References

- Blocklove, J., Garg, S., Karri, R., and Pearce, H. Chip-chat: Challenges and opportunities in conversational hardware design. In *5th ACM/IEEE Workshop on Machine Learning for CAD, MLCAD*. IEEE, 2023.
- Brayton, R. and Mishchenko, A. ABC: An academic industrial-strength verification tool. In *Computer Aided Verification: 22nd International Conference, CAV 2010, Edinburgh, UK, July 15–19, 2010. Proceedings 22*, pp. 24–40. Springer, 2010.
- Buchberger, B. and Loos, R. Algebraic simplification. In *Computer algebra: symbolic and algebraic computation*, pp. 11–43. Springer, 1982.
- Carette, J. Understanding expression simplification. In *Proceedings of the 2004 international symposium on Symbolic and algebraic computation*, pp. 72–79, 2004.
- Chang, K., Wang, Y., Ren, H., Wang, M., Liang, S., Han, Y., Li, H., and Li, X. Chipppt: How far are we from natural language hardware design. *CoRR*, abs/2305.14019, 2023.
- Chen, D. and Cong, J. Register binding and port assignment for multiplexer optimization. In *Proceedings of the 2004 Asia and South Pacific Design Automation Conference, ASP-DAC '04*, pp. 68–73. IEEE Press, 2004. ISBN 0780381750.
- Chu, P. P. *RTL hardware design using VHDL: coding for efficiency, portability, and scalability*. John Wiley & Sons, 2006.
- Cocke, J. Global common subexpression elimination. In *Proceedings of a symposium on Compiler Optimization*, pp. 20–24. ACM, 1970. doi: 10.1145/800028.808480.
- Cooper, K. D., Simpson, L. T., and Vick, C. A. Operator strength reduction. *ACM Transactions on Programming Languages and Systems (TOPLAS)*, 23(5):603–625, 2001.
- Deepa Tilwani, R. V. and Sheth, A. P. Neurosymbolic ai approach to attribution in large language models. *arXiv*, 2410.03726, September 2024. doi: 10.48550/arXiv.2410.03726. Paper under review.
- Diego Calanzone, S. T. and Vergari, A. Logically consistent language models via neuro-symbolic integration. *arXiv*, 2409.13724, September 2024. doi: 10.48550/arXiv.2409.13724.
- Fang, W., Lu, Y., Liu, S., Zhang, Q., Xu, C., Wills, L. W., Zhang, H., and Xie, Z. Masterrtl: A pre-synthesis ppa estimation framework for any rtl design. In *2023 IEEE/ACM International Conference on Computer Aided Design (ICCAD)*, pp. 1–9, 2023. doi: 10.1109/ICCAD57390.2023.10323951.
- Gupta, R., Benson, D., and Fang, J. Z. Path profile guided partial dead code elimination using predication. In *Proceedings 1997 International Conference on Parallel Architectures and Compilation Techniques*, pp. 102–113. IEEE, 1997.
- Hopcroft, J. E. and Ullman, J. D. *Formal languages and their relation to automata*. Addison-Wesley Longman Publishing Co., Inc., 1969.
- Hu, Y., Yang, H., Lin, Z., and Zhang, M. Code prompting: a neural symbolic method for complex reasoning in large language models, 2023. URL <https://arxiv.org/abs/2305.18507>.
- Knoop, J., Rüthing, O., and Steffen, B. Partial dead code elimination. *ACM Sigplan Notices*, 29(6):147–158, 1994.
- LaForest, C. E. and Steffan, J. G. Efficient multi-ported memories for fpgas. In *Proceedings of the 18th Annual ACM/SIGDA International Symposium on Field Programmable Gate Arrays (FPGA '10)*, pp. 41–50, Monterey, CA, USA, 2010. ACM. doi: 10.1145/1723112.1723122.
- Langley, P. Crafting papers on machine learning. In Langley, P. (ed.), *Proceedings of the 17th International Conference on Machine Learning (ICML 2000)*, pp. 1207–1216, Stanford, CA, 2000. Morgan Kaufmann.
- Liu, M., Ene, T., Kirby, R., Cheng, C., Pinckney, N. R., Liang, R., Alben, J., Anand, H., Banerjee, S., Bayraktaroglu, I., Bhaskaran, B., Catanzaro, B., Chaudhuri, A.,

- Clay, S., Dally, B., Dang, L., Deshpande, P., Dhodhi, S., Halepete, S., Hill, E., Hu, J., Jain, S., Khailany, B., Kunal, K., Li, X., Liu, H., Oberman, S. F., Omar, S., Pratty, S., Raiman, J., Sarkar, A., Shao, Z., Sun, H., Suthar, P. P., Tej, V., Xu, K., and Ren, H. Chipnemo: Domain-adapted llms for chip design. *CoRR*, abs/2311.00176, 2023a.
- Liu, M., Pinckney, N. R., Khailany, B., and Ren, H. Invited paper: Verilogval: Evaluating large language models for verilog code generation. In *IEEE/ACM International Conference on Computer Aided Design, ICCAD*. IEEE, 2023b.
- Liu, S., Fang, W., Lu, Y., Wang, J., Zhang, Q., Zhang, H., and Xie, Z. Rtlcoder: Fully open-source and efficient llm-assisted rtl code generation technique. *IEEE Transactions on Computer-Aided Design of Integrated Circuits and Systems*, 2024.
- Ma, J., Zuo, G., Loughlin, K., Cheng, X., Liu, Y., Eneyew, A. M., Qi, Z., and Kasikci, B. A hypervisor for shared-memory fpga platforms. In *Proceedings of the Twenty-Fifth International Conference on Architectural Support for Programming Languages and Operating Systems*, pp. 827–844, 2020.
- Moore, E. F. et al. Gedanken-experiments on sequential machines. *Automata studies*, 34:129–153, 1956.
- OpenAI, Achiam, J., Adler, S., Agarwal, S., Ahmad, L., Akkaya, I., Aleman, F. L., Almeida, D., Altenschmidt, J., Altman, S., Anadkat, S., Avila, R., Babuschkin, I., Balaji, S., Balcom, V., Baltescu, P., Bao, H., Bavarian, M., Belgum, J., Bello, I., Berdine, J., Bernadett-Shapiro, G., Berner, C., Bogdonoff, L., Boiko, O., Boyd, M., Brakman, A.-L., Brockman, G., Brooks, T., Brundage, M., Button, K., Cai, T., Campbell, R., Cann, A., Carey, B., Carlson, C., Carmichael, R., Chan, B., Chang, C., Chantzis, F., Chen, D., Chen, S., Chen, R., Chen, J., Chen, M., Chess, B., Cho, C., Chu, C., Chung, H. W., Cummings, D., Currier, J., Dai, Y., and many others. Gpt-4 technical report. *arXiv*, 2303.08774, March 2023. doi: 10.48550/arXiv.2303.08774. We report the development of GPT-4, a large-scale, multimodal model which exhibits human-level performance on various professional and academic benchmarks.
- Palnitkar, S. *Verilog HDL: a guide to digital design and synthesis*, volume 1. Prentice Hall Professional, 2003.
- Pasko, R., Schaumont, P., Derudder, V., Vernalde, S., and Duracková, D. A new algorithm for elimination of common subexpressions. *Computer-Aided Design of Integrated Circuits and Systems, IEEE Transactions on*, 18: 58 – 68, 02 1999. doi: 10.1109/43.739059.
- Schultz, J. Optimizing the rtl design flow with real-time ppa analysis. *Synopsys Silicon to Systems Blog*, N/A, March 2023. doi: N/A. Blog Post. URL: <https://www.synopsys.com/blogs/silicon-to-systems/optimizing-rtl-design-flow-real-time-ppa-analysis/> (Accessed January 26, 2025).
- Synopsys. Dc ultra for synthesis and test. <https://www.synopsys.com/implementation-and-signoff/rtl-synthesis-test/dc-ultra.html>.
- Takamaeda-Yamazaki, S. Pyverilog: A python-based hardware design processing toolkit for verilog hdl. In *Applied Reconfigurable Computing*, volume 9040 of *Lecture Notes in Computer Science*, pp. 451–460. Springer International Publishing, Apr 2015. doi: 10.1007/978-3-319-16214-0_42. URL http://dx.doi.org/10.1007/978-3-319-16214-0_42.
- Taraate, V. *Digital logic design using verilog*. Springer, 2022.
- Thakur, S., Ahmad, B., Pearce, H., Tan, B., Dolan-Gavitt, B., Karri, R., and Garg, S. Verigen: A large language model for verilog code generation. *ACM Trans. Design Autom. Electr. Syst.*, 2024.
- Tsai, Y., Liu, M., and Ren, H. Rtlfixer: Automatically fixing RTL syntax errors with large language model. In *Proceedings of the 61st ACM/IEEE Design Automation Conference, DAC*. ACM, 2024.
- Vahid, F. Digital design with rtl design, vhdl, and verilog (2nd edition). *John Wiley & Sons Inc*, 2, January 2010. doi: N/A. ISBN-13: 978-0470531082, 575 pages.
- Wan, Z., Liu, C.-f., Yang, H., Raj, R., Li, C., You, H., Fu, Y., Wan, C., Li, S., Kim, Y., Samajdar, A., Lin, Y., Ibrahim, M., Rabaey, J. M., Krishna, T., and Raychowdhury, A. Cross-layer design for neuro-symbolic ai: From workload characterization to hardware acceleration. *arXiv*, 2409.13153, September 2024a. doi: 10.48550/arXiv.2409.13153. Available at <https://arxiv.org/abs/2409.13153>.
- Wan, Z., Liu, C.-K., Yang, H., Raj, R., Li, C., You, H., Fu, Y., Wan, C., Li, S., Kim, Y., Samajdar, A., Lin, Y. C., Ibrahim, M., Rabaey, J. M., Krishna, T., and Raychowdhury, A. Towards efficient neuro-symbolic ai: From workload characterization to hardware architecture. *IEEE Transactions on Circuits and Systems for Artificial Intelligence*, 2409.13153, September 2024b. doi: 10.48550/arXiv.2409.13153.
- Wang, L.-T., Chang, Y.-W., and Cheng, K.-T. T. *Electronic design automation: synthesis, verification, and test*. Morgan Kaufmann, 2009.

- Wang, Z., You, H., Wang, J., Liu, M., Su, Y., and Zhang, Y. Optimization of multiplexer combination in rtl logic synthesis. In *Proceedings of the 2023 International Symposium of Electronics Design Automation (ISED)*, pp. N/A. IEEE, May 2023. doi: 10.1109/ISED59274.2023.10218464.
- Wolf, C., Glaser, J., and Kepler, J. Yosys-a free verilog synthesis suite. In *Proceedings of the Forum on Specification and Design Languages (FDL)*, 2013. URL <https://api.semanticscholar.org/CorpusID:202611483>. Yosys is the first open-source Verilog synthesis suite supporting a wide range of synthesizable Verilog features.
- Yang, S., Li, X., Cui, L., Bing, L., and Lam, W. Neuro-symbolic integration brings causal and reliable reasoning proofs. *arXiv*, 2311.09802, November 2023. doi: 10.48550/arXiv.2311.09802.
- Yao, X., Wang, Y., Li, X., Lian, Y., Ran, C., Chen, L., Yuan, M., Xu, H., and Yu, B. Rtlrewriter: Methodologies for large models aided rtl code optimization, 09 2024.
- Ye, J., Chen, X., Xu, N., Zu, C., Shao, Z., Liu, S., Cui, Y., Zhou, Z., Gong, C., Shen, Y., Zhou, J., Chen, S., Gui, T., Zhang, Q., and Huang, X. A comprehensive capability analysis of gpt-3 and gpt-3.5 series models, 2023. URL <https://arxiv.org/abs/2303.10420>.
- Zhou, H., Lin, Z., and Cao, W. Research on vhdl rtl synthesis system. In *Proceedings First IEEE International Workshop on Electronic Design, Test and Applications '2002*, pp. 99–103, 2002. doi: 10.1109/DELTA.2002.994596.

A FSM Symbolic System

The following section demonstrates an example FSM in verilog. First the verilog is transformed to Symbolic Representation, then the Symbolic system applied minimization algorithm to optimize the FSM.

```

1  module example(
2      input wire clk,
3      input wire reset,
4      input wire [1:0] input_signal,
5      output reg output_signal);
6      parameter S0 = 3'b000, S1 = 3'b001, S2 = 3'b010, S3 = 3'b011, S4 = 3'b100, S5 = 3'b101;
7      reg [2:0] current_state, next_state;
8      always @(current_state) begin
9          output_signal = 0;
10         case (current_state)
11             S0: output_signal = 1;
12             S2: output_signal = 1;
13             S4: output_signal = 1;
14             default: output_signal = 0;
15         endcase
16     end
17     always @(posedge clk or posedge reset) begin
18         if (reset) begin
19             current_state <= S0; // Reset to state S0
20         end else begin
21             current_state <= next_state;
22         end
23     end
24     always @(*) begin
25         next_state = current_state;
26         case (current_state)
27             S0: case (input_signal)
28                 2'b00: next_state = S0;
29                 2'b01: next_state = S1;
30                 2'b10: next_state = S2;
31                 2'b11: next_state = S3;
32             endcase
33             S1: case (input_signal)
34                 2'b00: next_state = S0;
35                 2'b01: next_state = S3;
36                 2'b11: next_state = S5;
37             endcase
38             S2: case (input_signal)
39                 2'b00: next_state = S1;
40                 2'b01: next_state = S3;
41                 2'b10: next_state = S2;
42                 2'b11: next_state = S4;
43             endcase
44             S3: case (input_signal)
45                 2'b00: next_state = S1;
46                 2'b01: next_state = S0;
47                 2'b10: next_state = S4;
48                 2'b11: next_state = S5;
49             endcase
50             S4: case (input_signal)
51                 2'b00: next_state = S0;
52                 2'b01: next_state = S1;
53                 2'b10: next_state = S2;
54                 2'b11: next_state = S5;
55             endcase
56             S5: case (input_signal)
57                 2'b00: next_state = S1;
58                 2'b01: next_state = S4;
59                 2'b10: next_state = S0;
60             endcase
61         endcase
62     end
63 endmodule

```

Listing 1: Example Test Case: example1_state.


```

1  'states': ['S0', 'S1', 'S2', 'S3', 'S4', 'S5'],
2  'transitions': {
3      'S0': {
4          'input_signal=00': {'next_state': 'S0'},
5          'input_signal=01': {'next_state': 'S1'},
6          'input_signal=10': {'next_state': 'S2'},
7          'input_signal=11': {'next_state': 'S3'}
8      },
9      'S1': {
10         'input_signal=00': {'next_state': 'S0'},
11         'input_signal=01': {'next_state': 'S3'},
12         'input_signal=11': {'next_state': 'S5'}
13     },
14     'S2': {
15         'input_signal=00': {'next_state': 'S1'},
16         'input_signal=01': {'next_state': 'S3'},
17         'input_signal=10': {'next_state': 'S2'},
18         'input_signal=11': {'next_state': 'S4'}
19     },
20     'S3': {
21         'input_signal=00': {'next_state': 'S1'},
22         'input_signal=01': {'next_state': 'S0'},
23         'input_signal=10': {'next_state': 'S4'},
24         'input_signal=11': {'next_state': 'S5'}
25     },
26     'S4': {
27         'input_signal=00': {'next_state': 'S0'},
28         'input_signal=01': {'next_state': 'S1'},
29         'input_signal=10': {'next_state': 'S2'},
30         'input_signal=11': {'next_state': 'S5'}
31     },
32     'S5': {
33         'input_signal=00': {'next_state': 'S1'},
34         'input_signal=01': {'next_state': 'S4'},
35         'input_signal=10': {'next_state': 'S0'}
36     }
37 },
38 'outputs': {'S0': {'output_signal': 1},
39             'S1': {'output_signal': 0},
40             'S2': {'output_signal': 1},
41             'S3': {'output_signal': 0},
42             'S4': {'output_signal': 1},
43             'S5': {'output_signal': 0}}

```

Listing 2: LLM-generated symbolic representation for example1_state.

```

1  State: S2, Output: 1
2      input_signal=00 -> S1
3      input_signal=01 -> S3_S5
4      input_signal=10 -> S2
5      input_signal=11 -> S0_S4
6  State: S0_S4, Output: 1
7      input_signal=00 -> S0_S4
8      input_signal=01 -> S1
9      input_signal=10 -> S2
10     input_signal=11 -> S3_S5
11 State: S1, Output: 0
12     input_signal=00 -> S0_S4
13     input_signal=01 -> S3_S5
14     input_signal=10 -> S1
15     input_signal=11 -> S3_S5
16 State: S3_S5, Output: 0
17     input_signal=00 -> S1
18     input_signal=01 -> S0_S4
19     input_signal=10 -> S0_S4
20     input_signal=11 -> S3_S5

```

Listing 3: Reduced states of example1_state.

B AST Template

The following section demonstrate how applying AST templates transforms the code and apply optimization patterns.

```

1 module example_raw
2   #( parameter BW = 8)
3   (
4     input [BW-1:0] a,
5     input [BW-1:0] b,
6     input [BW-1:0] c,
7     input [BW-1:0] d,
8     output [BW-1:0] s1
9   );
10  assign s2 = a * b;
11  assign s3 = a % b + d;
12  assign s4 = c + d + b * a;
13  assign s5 = a - b;
14  assign s6 = (b + 1) * a + d + c - b;
15  assign s1 = a + 23;
16 endmodule

```

Listing 4: Example Test Case: dead_code_elimination.

```

1 module example_raw #
2   (parameter BW = 8)
3   (
4     input [BW-1:0] a,
5     input [BW-1:0] b,
6     input [BW-1:0] c,
7     input [BW-1:0] d,
8     output [BW-1:0] s1
9   );
10  assign s1 = a + 23;
11 endmodule

```

Listing 5: Example Test Case: dead_code_elimination after applying the Dead Code Elimination AST template.

```

1 module example_raw
2   #( parameter BW = 8)
3   (
4     input [BW-1:0] a,
5     input [BW-1:0] b,
6     input [BW-1:0] c,
7     input [BW-1:0] d,
8     output [BW-1:0] s1,
9     output [BW-1:0] s2,
10    output [BW-1:0] s3,
11    output [BW-1:0] s4,
12    output [BW-1:0] s5,
13    output [BW-1:0] s6
14  );
15  assign s1 = a + b;
16  assign s2 = a * b;
17  assign s3 = a \% b + d;
18  assign s4 = c + d + b * a;
19  assign s5 = a - b;
20  assign s6 = (b + 1) * a + d + c - b;
21 endmodule

```

Listing 6: Example Test Case: subexpression_elimination.

```

1 module example
2   #( parameter      BW = 8)
3   (
4     input [BW-1:0] a,
5     input [BW-1:0] b,
6     input [BW-1:0] c,
7     input [BW-1:0] d,
8     output [BW-1:0] s1,
9     output [BW-1:0] s2,
10    output [BW-1:0] s3,
11    output [BW-1:0] s4,
12    output [BW-1:0] s5,
13    output [BW-1:0] s6
14  );
15  assign s1 = a + b;
16  assign s2 = a * b;
17  assign s3 = a \% b + d;
18  assign s4 = c + d + s2;
19  assign s5 = a - b;
20  assign s6 = s4 + s5;
21 endmodule

```

Listing 7: Example Test Case: subexpression_elimination after applying the Common Sub-Expressions Elimination template. The Common Sub-Expressions are reused in the states after it.

```

1 module example_raw
2   #( parameter      BW = 8)
3   (
4     input [BW-1:0] a,
5     input [BW-1:0] b,
6     output [BW-1:0] s1,
7     output [BW-1:0] s2
8   );
9   wire [BW-1:0] t1, t2;
10  assign s1 = a + b;
11  assign t1 = s1 + 0;
12  assign t2 = s1 * 1;
13  assign s2 = t1 + t2;
14 endmodule

```

Listing 8: Example Test Case: algebraic_simplification.

```

1 module example_raw #
2   (
3     parameter BW = 8
4   )
5   (
6     input [BW-1:0] a,
7     input [BW-1:0] b,
8     output [BW-1:0] s1,
9     output [BW-1:0] s2
10  );
11
12  assign s1 = a + b;
13  assign s2 = s1 + s1;
14
15 endmodule
16

```

Listing 9: Example Test Case: algebraic_simplification after applying the Temporary Variable Elimination, Dead Code Elimination, then Expression Simplification templates.

C RAG Example

Sample Retrieval Augmented Optimization Rule

```
"name" : "Zero Multiplication Elimination",
"pattern" : "Detect multiplication by zero in expressions (e.g., , 0 * c)",
"rewrite" : "Eliminate multiplication by zero, replacing the entire expression with zero",
"category" : "combinational/dataflow",
"objective_improvement" : "area",
"template_guidance" : "Identify vast.Times nodes with a zero operand. Replace the node with a vast.IntConst node representing zero.",
"function_name" : "ZeroMultiplicationTemplate"
```

Figure 6. Sample Retrieval Augmented Optimization Rule 1: Zero Multiplication Rule.

Sample Retrieval Augmented Optimization Rule

```
"name" : "IntermediateVariableExtraction",
"pattern" : "Detect conditional assignments to a register based on a control signal",
"rewrite" : "Extract common sub-expressions into intermediate variables to reduce redundant logic",
"category" : "combinational/dataflow",
"objective_improvement" : "area",
"template_guidance" : "To implement this rule in a Python template subclassing BaseTemplate, use pyverilog AST manipulation to identify conditional assignments (vast.IfStatement) and extract the common sub-expressions into separate assignments. Look for vast.Identifier nodes that are assigned conditionally and create new vast.Assign nodes for the intermediate variables. Ensure that the new assignments are placed before the conditional logic to maintain correct data flow",
"function_name" : "IntermediateVariableExtractionTemplate"
```

Figure 7. Sample Retrieval Augmented Optimization Rule 2: Intermediate Variable Extraction.

Hardware Optimization Rule

```
"name" : "ReplaceRippleCarryWithCarryLookahead",
"pattern" : "Detects a ripple carry adder implementation using a series of full adders connected in sequence",
"rewrite" : "Transforms the ripple carry adder into a carry lookahead adder by using partial full adders and generating carry bits in parallel",
"category" : "combinational/dataflow",
"objective_improvement" : "area, delay",
"template_guidance" : null,
"function_name" : null
```

Figure 8. Sample Retrieval Augmented Optimization Rule 3: Replace Ripple Carry with Carry Lookahead, no template guidance is needed since it is an abstract rule.